

Direct measurement of single fluxoid dynamics in superconducting rings

J. R. Kirtley and C. C. Tsuei

IBM T.J. Watson Research Center, P.O. Box 218, Yorktown Heights, NY 10598

H. Raffy and Z. Z. Li

Laboratoire de Physique des Solides, Université Paris-Sud, 91405 Orsay, France

V. G. Kogan and J. R. Clem

Ames Laboratory and Department of Physics and Astronomy, Iowa State University, Ames, IA 50011

K. A. Moler

Dept. of Applied Physics, Stanford University, Stanford, CA 94305

(November 13, 2018)

We have measured the dynamics of individual magnetic fluxoids entering and leaving photolithographically patterned thin film rings of underdoped high-temperature superconductor $\text{Bi}_2\text{Sr}_2\text{CaCu}_2\text{O}_{8+\delta}$, using a variable sample temperature scanning SQUID microscope. These measurements can be understood within a phenomenological model in which the fluxoid number changes by thermal activation of a Pearl vortex in the ring wall. We place upper limits on the “vison” binding energy in these samples from these measurements.

Although there is a vast literature on vortex dynamics in superconductors [1], with a few notable exceptions [2,3] this work has involved indirect measurements of collective motions of vortices through, to cite a few recent examples, transport [4–7], voltage noise [8], magnetization loops [9], persistent currents in rings [10,11], or microwave impedance [12]. In this Letter, we present direct measurements of the dynamics of individual magnetic fluxoids leaving and entering superconducting rings with a well defined geometry. These measurements represent a new tool for studying vortex dynamics.

Our measurements were made on 300 nm thick films of the high-temperature superconductor $\text{Bi}_2\text{Sr}_2\text{CaCu}_2\text{O}_{8+\delta}$ (BSCCO), epitaxially grown on (100) SrTiO_3 substrates using magnetron sputtering. The oxygen concentration in these films was varied by annealing in oxygen or argon at 400–450 °C. The films were photolithographically patterned into circular rings using ion etching. The rings had outside diameters of 40, 60, and 80 μm , with inside diameters half the outside diameters. The film for the current measurements had a broad resistive transition (90% of the extrapolated normal state resistance at $T=79$ K, 10% at $T=46$ K) with a zero-resistance T_c of 36 K before patterning. After patterning the rings had T_c ’s from 25 K to 33 K, as indicated by inductive measurements. The rings were magnetically imaged using a variable sample temperature scanning Superconducting Quantum Interference Device (SQUID) microscope [13], which scans a sample relative to a SQUID with a small, well shielded, integrated pickup loop (a square loop 17.8 μm on a side for these measurements), the sample temperature being varied while the low- T_c SQUID remains superconducting. Figure 1(a) shows a scanning SQUID microscope image of some of these rings, cooled in a magnetic field

sufficient to trap one vortex in each ring. The dots in Figure 1(b) are a cross-section through the center of one ring. The curve in Figure 1(b) is modeled as follows:

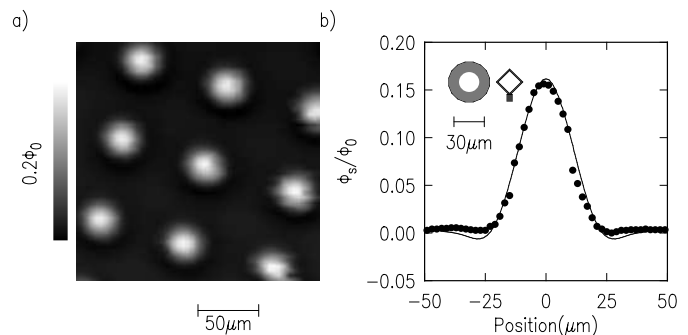


FIG. 1. (a) Scanning SQUID microscope image of 40 μm diameter rings cooled in a field of 30 mG, and imaged in zero field at $T=10.5$ K. Each ring has one fluxoid trapped in it. (b) Cross-section through the center of the central ring in (a) (dots), and modelling as described in the text (line). The insets show schematics of the ring and SQUID pickup loop geometries. Φ_s is the flux through the SQUID pickup loop.

Consider a thin film ring of thickness $d \ll \lambda_L$ (the London penetration depth) with radii $a < b$ in the plane $z = 0$. The London equations for the film interior read

$$\mathbf{j} = -\frac{c\Phi_0}{8\pi^2\lambda_L^2} \left(\nabla\theta + \frac{2\pi}{\Phi_0} \mathbf{A} \right), \quad (1)$$

where \mathbf{j} is the supercurrent density, $\Phi_0 = hc/2e$ is the superconducting flux quantum, θ is the order parameter phase, and \mathbf{A} is the vector potential. Since the current in the ring must be single valued, $\theta = -N\varphi$, where φ is the azimuth and the integer N is the winding number (vorticity) of the state. Integrating \mathbf{j} over the film thickness d , we obtain:

$$g_\varphi \equiv g(r) = \frac{c\Phi_0}{4\pi^2\Lambda} \left(\frac{N}{r} - \frac{2\pi}{\Phi_0} A_\varphi \right), \quad (2)$$

where $g(r)$ is the sheet current density directed along the azimuth φ , and $\Lambda = 2\lambda_L^2/d$ is Pearl's film penetration depth [14]. The vector potential A_φ can be written as

$$A_\varphi(r) = \int_a^b d\rho g(\rho) a_\varphi(\rho; r, 0) + \frac{r}{2} H, \quad (3)$$

where the last term represents a uniform applied field H in the z direction and $a_\varphi(\rho; r, z)$ is the vector potential of the field created by a circular unit current of a radius ρ : [15]

$$a_\varphi(\rho; r, z) = \frac{4}{ck} \sqrt{\frac{\rho}{r}} \left[\left(1 - \frac{k^2}{2} \right) \mathbf{K}(k) - \mathbf{E}(k) \right],$$

$$k^2 = \frac{4\rho r}{(\rho + r)^2 + z^2}. \quad (4)$$

Here, $\mathbf{K}(k)$ and $\mathbf{E}(k)$ are the complete elliptic integrals in the notation of Ref. [16].

Substituting Eq. (3) and (4) into (2), we obtain an integral equation for $g(r)$:

$$\frac{4\pi^2\Lambda}{c} r g(r) + \pi r^2 H - \Phi_0 N$$

$$= -\frac{4\pi}{c} \int_a^b d\rho g(\rho) \left[\frac{\rho^2 + r^2}{\rho + r} \mathbf{K}(k_0) - (\rho + r) \mathbf{E}(k_0) \right], \quad (5)$$

where $k_0^2 = 4\rho r/(\rho + r)^2$. This equation is solved by iteration for a given integer N and field H to produce current distributions which we label as $g_N(H, r)$.

After $g_N(H, r)$ is found, the field outside the ring can be calculated using Eq. (4):

$$h_z(N; r, z) = \frac{2}{c} \int_a^b \frac{d\rho g_N(H, \rho)}{\sqrt{(\rho + r)^2 + z^2}} \left[\mathbf{K}(k) \right.$$

$$\left. + \frac{\rho^2 - r^2 - z^2}{(\rho - r)^2 + z^2} \mathbf{E}(k) \right] + H. \quad (6)$$

The flux through the SQUID is obtained numerically by integrating Eq. (6) over the pickup loop area. The line in Fig. 1b is a two parameter fit of this integration of Eq. (6) to the data, resulting in $z=3.5 \mu\text{m}$, and $\Lambda=9 \mu\text{m}$ (corresponding to $\lambda_L=1.1 \mu\text{m}$).

The fluxoid number N of a ring could be changed by varying an externally applied flux $\Phi_a = A_{eff}H$, $A_{eff} \approx \pi(a^2 + b^2)/2$ [18], and monitored by positioning the SQUID pickup loop directly over it [19]. We always observed single fluxoid switching events, as determined by the agreement (to within 10%) of the measured spacing in applied flux between vortex switching events with our calculations for $|\Delta N| = 1$, in the experiments reported here. Switching distributions $P(\Phi_{a,i})$ were obtained by repeatedly sweeping the applied field, in analogy with experiments on Josephson junctions [20]. The

transition rates ν of the fluxoid states were determined from this data using

$$\nu(\Phi_{a,m}) = \frac{d\Phi_a/dt}{\Delta\Phi_a} \ln \left\{ \frac{\sum_{j=1}^m P(\Phi_{a,j})}{\sum_{i=1}^{m-1} P(\Phi_{a,i})} \right\}, \quad (7)$$

where $m = 1$ labels the largest Φ_a in a given switching histogram peak [20], and $\Delta\Phi_a$ is the flux interval between data points.

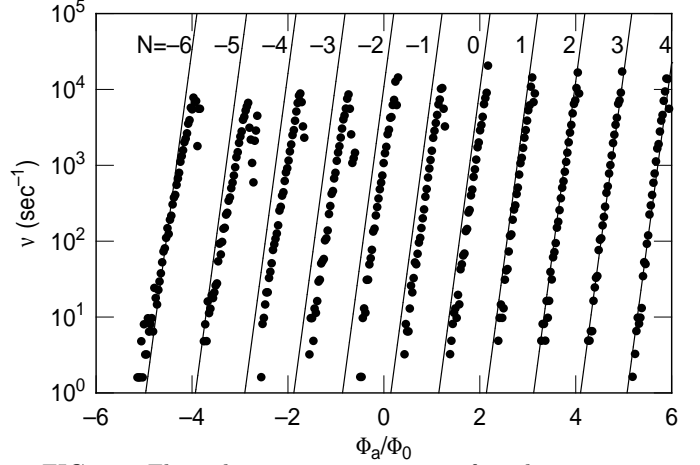


FIG. 2. Fluxoid transition rates ν for the transition $N \rightarrow N + 1$ vs. the externally applied flux Φ_a (swept towards positive Φ_a) for a BSCCO ring of $80 \mu\text{m}$ outer diameter, with $T_c=32.5 \text{ K}$, at a temperature of 30.9 K . The dots are experiment; the lines are the model described in the text.

The dots in Figure 2 show the results from one such experiment. The lines are from a phenomenological model (a full theory will be published elsewhere): We take the energy of the ring in its initial or final state to be [21]

$$E_r(N) = \frac{\Phi_0^2}{2L} (N - \phi_a)^2, \quad (8)$$

where $\phi_a = \Phi_a/\Phi_0$, and L is the inductance of the ring. We take the ring maximum energy during the transition $N \rightarrow N'$ to be

$$E_t(N, N') = E_V - \alpha(N + N')^2/4 + (E_r(N) + E_r(N'))/2, \quad (9)$$

where the first two terms on the right hand side represent the energy required to nucleate a vortex in the ring wall. The maximum vortex energy in a straight thin film superconducting strip of width $W \ll \Lambda$ (carrying no transport supercurrent) is [22]

$$E_V = \frac{\Phi_0^2}{8\pi^2\Lambda} \ln \left\{ \frac{2W}{\pi\xi} \right\}. \quad (10)$$

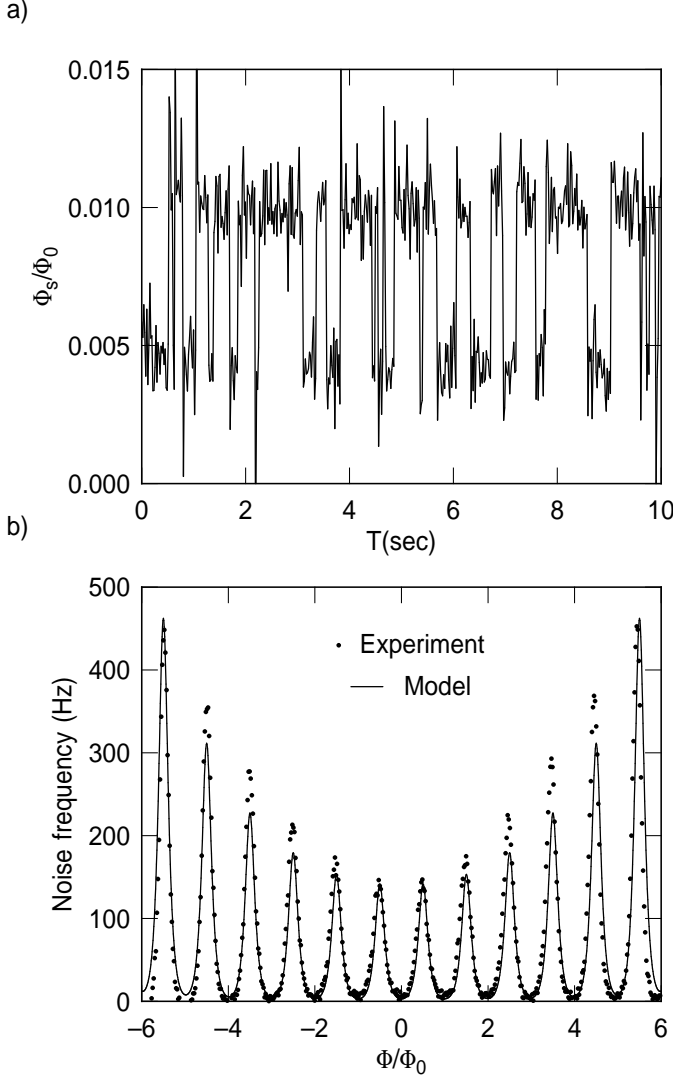


FIG. 3. a) Telegraph noise signal vs. time for the ring of Figure 2 at $T=31.4$ K, $\Phi_a = \Phi_0/2$. b) Telegraph noise frequency vs externally applied field Φ_a/Φ_0 for telegraph noise of this ring at $T=31.6$ K.

Since $\lambda_L \propto 1/\sqrt{1-t^4}$ ($t = T/T_c$) [24], we take $E_V = E_{V0}(1 - t^4)$. α is a fitting parameter which describes the reduction of the vortex nucleation energy with increasing N . For thermal activation, the $N \rightarrow N'$ transition rate is $\nu = \nu_0 e^{-E_a(N, N')/k_B T}$, where ν_0 is an attempt frequency and the activation energy $E_a(N, N') = E_t(N, N') - E_r(N)$. For this ring (from fits to the data of Fig.'s 2, 3 and 4) we take $E_{V0} = 6 \times 10^{-13}$ erg, $\alpha = 1.7 \times 10^{-16}$ erg, and $\Phi_0^2/2L = 4.6 \times 10^{-14}$ erg. Taking $\Lambda = 200 \mu m$ at $T=31.5$ K from fits of Eq. (6) to SSM data, $\xi = 3.2/\sqrt{1-t}$ nm, and $W = 20 \mu m$, we find $E_{V0} = 1.55 \times 10^{-12}$ erg, a factor of 2.6 larger than the 6×10^{-13} erg from our fits. It has been proposed that surface defects could reduce the barrier to entry of vortices in type-II superconductors [23]. If we calculate an effective inductance for the ring as $L^* = \Phi_0/I_s$,

where $I_s = \int_a^b dr g_N(H; r)$, and use the solution of Eq. (5) for $N = 1$, $H = 0$, and $\Lambda = 200 \mu m$, we find $\Phi_0^2/2L^* = 1.8 \times 10^{-14}$ erg, a factor of 2.6 smaller than the 4.6×10^{-14} erg from our fit. For ring temperatures close to T_c , telegraph noise (Figure 3a) from thermally activated switching $N \leftrightarrow N'$ occurs. This noise peaks when $\Phi_a = (N + 1/2)\Phi_0$, N an integer. Figure 3b shows the telegraph noise frequency (number of steps up per sec) as a function of applied field for the ring of Figure 2 at a temperature $T=31.6$ K. The line is the prediction of the model described above, using the same fitting parameters, and writing the telegraph noise frequency as [25]

$$\nu = 2\nu_0 \frac{e^{-E_{in}/k_B T} e^{-E_{out}/k_B T}}{e^{-E_{in}/k_B T} + e^{-E_{out}/k_B T}}, \quad (11)$$

where $E_{in} = E_a(N, N + 1)$ and $E_{out} = E_a(N + 1, N)$. Finally, the symbols in Figure 4 show the telegraph noise frequency for the same ring as in Figures 2 and 3, as a function of temperature with $\Phi_a = \Phi_0/2$. The line is the prediction of our simple model, with the same fitting parameters as above.

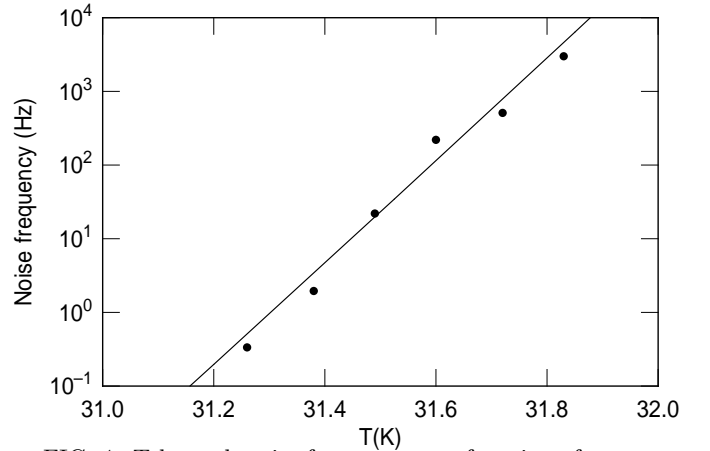


FIG. 4. Telegraph noise frequency as a function of temperature, with $\Phi_a = \Phi_0/2$ for the ring of Figures 2 and 3 (dots). The line is the prediction of the model discussed in the text.

The data shown in Figures 2, 3, and 4 are all consistent with an attempt frequency $\nu_0 \sim 3 \times 10^8 \text{ sec}^{-1}$. Glazman and Fogel [26], in a treatment of quantum tunneling of vortices, write $\nu_0 = \sqrt{\Phi_0 B_{c2}/4\pi\Lambda m}$, where the vortex mass $m = \hbar\eta/\Delta$, and the damping parameter $\eta = \Phi_0 B_{c2} d/\rho_n c^2$. Taking the second critical field B_{c2} equal to 1 T for $T_c - T = 1$ K, the normal state sheet resistivity $\rho_n = 1200 \mu\Omega\text{-cm}$, and $\Delta = 5k_B T_c = 2.24 \times 10^{-14}$ erg, we find $\nu_0 = 9.7 \times 10^8 \text{ sec}^{-1}$, within a factor of three of our measurements. A second estimate, in a treatment of thermal activation of vortices [27], is $\nu_0 = 6.96(D/a^2)\sqrt{E_V/k_B T}$, where the diffusion constant $D = k_B T/\eta$. Using $a = 40 \mu m$, and the other parameters the same as before, this expression gives $\nu_0 = 1.5 \times 10^5 \text{ sec}^{-1}$. The disparity between these two estimates provides a measure of the uncertainties involved

in calculating attempt frequencies.

Senthil and Fisher [28] and Sachdev [29] have proposed tests of the idea that the electron is fractionalized in the high- T_c cuprate superconductors. The Senthil-Fisher proposal is to look for persistence of vorticity in underdoped cuprate cylinders as they are cycled through the superconducting transition temperature. This experiment has been performed by Bonn *et al.* [30] on single crystals of $\text{YBa}_2\text{Cu}_3\text{O}_{6.3}$, and by us on the present ring samples, with no evidence to date for this persistent vorticity. The predicted effect depends on the existence of a gapped topological excitation, dubbed a “vison”, that is associated with a conventional vortex below the superconducting transition temperature, but which persists up to the pseudogap temperature. The present experiments provide another test of these ideas. It has been proposed that the vison should have a binding energy above the superconducting transition temperature of order $E_{\text{vison}} \sim k_B T^*$ [28]. The pseudogap temperature T^* is estimated to be approximately 300 K [31] for BSCCO with a T_c of 30 K. If we assume that the vortex thermal activation energy at T_c is equal to the vison binding energy E_{vison} (since the vortex core and supercurrent contributions to the vortex energy have gone to zero), then the telegraph noise frequency extrapolated to T_c should be given by $\nu(T = T_c) = \nu_0 e^{-E_{\text{vison}}/k_B T_c}$, or $E_{\text{vison}} = k_B T_c \ln(\nu_0/\nu(T = T_c))$. The larger of our two estimates for the attempt frequency ν_0 would lead to $E_{\text{vison}}/k_B \sim 60\text{K}$. The smaller estimate would indicate a smaller binding energy. A conservative estimate for an upper limit of the attempt frequency would be $\nu_0 \sim c/b = 4 \times 10^{12} \text{ sec}^{-1}$, where c is the speed of light, and b is the outer radius of the ring, which would lead to an upper limit for $E_{\text{vison}}/k_B \sim 300 \text{ K}$.

In conclusion, we have demonstrated a technique for measuring the dynamics of single vortices on a relatively short time scale, limited by the modulation frequency (100KHz) of our SQUID electronics (modulation frequencies 10^3 times faster have been demonstrated). These measurements were made possible by using cuprate superconductors that were highly underdoped, so that the penetration depths were longer than the ring wall lengths, and the vortex activation energies were comparable to the temperature, over an appreciable temperature range below T_c . Although these measurements were apparently made in a regime where the fluxoid transitions were mediated by thermally activated Pearl vortices, it may be possible to use similar techniques to study single vortex tunneling [26].

We would like to thank T. Senthil and M.P.A. Fisher for suggesting these experiments to us, and R. Koch, S. Woods, D. Bonn, W.A. Hardy, D.J. Scalapino, and F. Tafuri for useful conversations. Ames Laboratory is operated for the U.S. Department of Energy by Iowa State

University under Contract No. W-7405-Eng-82. This research was supported by the Director for Energy Research, Office of Basic Energy Sciences.

-
- [1] G. Blatter *et al.*, Rev. Mod. Phys. **66**, 1125 (1994).
 - [2] K. Harada *et al.*, Science **274**, 1167 (1996).
 - [3] B.L.T. Plourde and D.J. van Harlingen, *Physics and Materials Science of Vortex States, Flux Pinning and Dynamics*, Proceedings of the Nato Advanced Study Institute, 1991, p. 281.
 - [4] M. Pannetier *et al.*, Phys. Rev. B **62**, 15162 (2000).
 - [5] W.K. Park and Z.G. Khim, Phys. Rev. B **61**, 1530 (2000).
 - [6] Y. Paltiel *et al.*, Nature **403**, 398 (2000).
 - [7] S.N. Gordeev *et al.*, Nature **385**, 324 (1997).
 - [8] S. Okuma and N. Kokubo, Phys. Rev. B **61**, 671 (2000).
 - [9] G.K. Perkins and A.D. Caplin, Phys. Rev. B **54**, 12551 (1996).
 - [10] H. Darhmaoui and J. Jung, Phys. Rev. B **57**, 8009 (1998).
 - [11] H. Yan *et al.*, Phys. Rev. B **61**, 11711 (2000).
 - [12] Y.M. Habib *et al.*, Phys. Rev. B **57**, 13833 (1998).
 - [13] J.R. Kirtley *et al.*, Appl. Phys. Lett. **74**, 4011 (1999).
 - [14] J. Pearl, J. Appl. Phys. **37**, 4139 (1966).
 - [15] L. D. Landau and E. M. Lifshitz, *Electrodynamics of Continuous Media*, Pergamon, NY, 1984.
 - [16] I. S. Gradshteyn and I. M. Ryzhik, *Tables of Integrals*, Academic Press, NY, 1980.
 - [17] T.A. Fulton and L.N. Dunkelberger, Phys. Rev. B **9**, 4760 (1974).
 - [18] M.B. Ketchen *et al.*, *SQUID '85: Superconducting Quantum Interference Devices and Their Applications*, ed. H.D. Hahlbohm and H. Lübbig, Walter de Gruyter, Berlin, 1985, p. 865.
 - [19] C.C. Tsuei *et al.*, Phys. Rev. Lett. **73**, 593 (1994).
 - [20] T.A. Fulton and L.N. Dunkelberger, Phys. Rev. B **9**, 4760 (1974).
 - [21] A. Barone and G. Paterno, *Physics and Applications of the Josephson Effect*, Wiley, New York, 1982, p. 355.
 - [22] V.G. Kogan, Phys. Rev. B **49**, 15874 (1994). Although this paper has an error, the results are correct for ring sizes small relative to the Pearl length.
 - [23] D. Yu. Vodolazov, I.L. Maksimov, and E.H. Brandt, cond-mat/0101074 (2001).
 - [24] M. Tinkham, *Introduction to Superconductivity*, McGraw-Hill, New York, 1975, p. 80.
 - [25] S. Machlup, J. Appl. Phys. **25**, 341 (1954).
 - [26] L.I. Glazman and N. Ya. Fogel', Sov. J. Low. Temp. Phys. **10**, 51 (1984).
 - [27] J.R. Clem, unpublished.
 - [28] T. Senthil and M.P.A. Fisher, Phys. Rev. Lett. **86**, 292 (2001).
 - [29] S. Sachdev, cond-mat/009456 (2000).
 - [30] D.A. Bonn *et al.*, preprint.
 - [31] Z. Konstantinovic, Z.Z. Li, and H. Raffy, Physica B **259-261**, 567 (1999).